A Role for the Basal Forebrain Cholinergic System in Estrogen-Induced Disinhibition of Hippocampal Pyramidal Cells

Charles N. Rudick,[1] Robert B. Gibbs,[2] and Catherine S. Woolley[1]

[1]Department of Neurobiology and Physiology and Northwestern University Institute for Neuroscience, Northwestern University, Evanston, Illinois 60208, and [2]Department of Pharmaceutical Sciences, University of Pittsburgh, Pittsburgh, Pennsylvania 15261

Estrogen transiently disinhibits hippocampal CA1 pyramidal cells in adult female rats and prolongs the decay time of IPSCs in these cells. Estrogen-induced changes in synaptic inhibition are likely to be causally related to subsequent enhancements in excitatory synaptic function in CA1 pyramidal cells. Currently, it is unknown how or on what cells estrogen acts to regulate synaptic inhibition in the hippocampus. We used whole-cell voltage-clamp recording of synaptically evoked IPSCs, spontaneous IPSCs, and miniature IPSCs in CA1 pyramidal cells to evaluate estrogen-induced changes in synaptic inhibition in ovariectomized rats that either were pretreated with the estrogen receptor (ER) antagonist tamoxifen or in which basal forebrain cholinergic neurons were eliminated by previous infusion of 192IgG-saporin toxin into the medial septum. We found that estrogen-induced disinhibition and prolongation of IPSCs are entirely dependent on a tamoxifen-sensitive ER. Estrogen-induced disinhibition is partially dependent on basal forebrain cholinergic neurons, but the prolongation of IPSCs is not at all dependent on these cells. Paired-pulse experiments and recordings of action potential-related spontaneous IPSCs suggest that estrogen-induced disinhibition is associated with a decrease in probability of release at GABAergic synapses, which decreases the amplitude of IPSCs produced by inhibitory neuron action potentials. Our findings lend novel insights into estrogen regulation of inhibitory synapses in the hippocampus and point to estrogen action on basal forebrain cholinergic neurons as critically involved in mediating the effects of estrogen in the hippocampus.

Key words: GABA; IPSCs; tamoxifen; ChAT; estradiol; 192IgG-saporin; CA1

Introduction

Estrogen regulates both inhibitory and excitatory synaptic input to CA1 pyramidal cells in the hippocampus of adult female rats. With a relatively short latency of 24 hr, estrogen decreases the amplitude of synaptically evoked GABA$_A$ receptor-mediated IPSCs and decreases the frequency, but not amplitude, of miniature IPSCs (mIPSCs) in these cells (Rudick and Woolley, 2001). The decrease in inhibitory synaptic function induced by estrogen is transient in that by 72 hr, inhibition is restored to control levels. In parallel with the restoration of inhibition, excitatory input to CA1 pyramidal cells is enhanced: dendritic spine and synapse density are increased (Woolley and McEwen, 1992), NMDA receptor function is enhanced (Rudick and Woolley, 2001), and spatial working memory is improved (Daniel and Dohanich, 2001; Sandstrom and Williams, 2001). On the basis of *in vitro* studies (Murphy et al., 1998), the transient suppression of GABAergic inhibition induced by estrogen is likely to be a causal factor in subsequent enhancement of excitatory input to hippocampal pyramidal cells.

Estrogen also transiently alters the kinetics of CA1 pyramidal cell IPSCs at the same time that it decreases IPSC amplitude.

Twenty-four hours after estrogen, synaptically evoked IPSCs show a prolonged decay time, which is paralleled by the appearance of a subpopulation of mIPSCs with prolonged decay. By 72 hr, evoked IPSC decay has returned to control levels, and the subpopulation of prolonged mIPSCs has disappeared.

Currently, it is unknown how or where estrogen acts to regulate synaptic inhibition in the hippocampus. Estrogen can act through classical nuclear receptors, estrogen receptor (ER)-α and ER-β, and through "rapid effects" that may involve membrane or cytoplasmic receptors (Moss and Gu, 1999). CA1 pyramidal cells lack classical ERs; however, ER-α is expressed in a subset of GABAergic neurons in CA1 (Hart et al., 2001), as well as in afferents to the hippocampus. Basal forebrain cholinergic neurons in particular are good candidates for involvement in the effects of estrogen in the hippocampus: ~37% of cholinergic neurons in the medial septum bind estrogen and express ER-α (Shughrue et al., 2000), estrogen increases basal forebrain choline acetyltransferase activity (Luine, 1985), high-affinity choline uptake (Gibbs, 2000), and acetylcholine release (Gibbs et al., 1997), and at least some of the effects of estrogen on hippocampal excitatory synaptic function are blocked by an M2 muscarinic receptor antagonist (Daniel and Dohanich, 2001).

To begin to elucidate the mechanisms by which estrogen regulates synaptic inhibition in the hippocampus, we tested whether the ER antagonist tamoxifen can block the effects of estrogen on CA1 pyramidal cell IPSCs and the ability of estrogen to regulate IPSCs in animals in which basal forebrain cholinergic neurons were eliminated by infusion of 192IgG-saporin (Sap) toxin into

the medial septum. Our findings demonstrate that estrogen regulation of hippocampal synaptic inhibition depends completely on tamoxifen-sensitive ERs and partly on basal forebrain cholinergic neurons. We propose models for estrogen action in the basal forebrain to disinhibit hippocampal pyramidal cells.

Materials and Methods

Animal treatments. Animal procedures were approved by the Northwestern University Animal Care and Use Committee. Adult female Sprague Dawley rats (180–220 gm) were housed on a 12 hr light/dark cycle with *ad libitum* access to food and water. All rats were bilaterally ovariectomized under ketamine (85 mg/kg)/xylazine (13 mg/kg) anesthesia using aseptic procedures. On the third day after surgery, rats were injected subcutaneously with either 10 μg of 17β-estradiol benzoate (E) in 100 μl of sesame oil or 100 μl of sesame oil (O) alone. For pretreatment with tamoxifen, rats received 2 mg/kg tamoxifen (T) or oil vehicle (V) 12 hr before and concurrently with the E or O injections. Twenty-four hours after E or O injection, animals were killed for preparation of hippocampal slices.

In additional experiments, 192IgG-Sap (Chemicon International, Temecula, CA) was infused directly into the medial septum to selectively destroy basal forebrain cholinergic neurons before ovariectomy. 192IgG-Sap is a selective immunotoxin consisting of the ribosome-inactivating toxin saporin coupled to an antibody against the p75NTR. Infusing small quantities of Sap directly into the medial septum selectively destroys cholinergic projection neurons, with no apparent affect on GABAergic projections (Book et al., 1994; Gibbs, 2002; Johnson et al., 2002). Infusions were performed as described recently (Johnson et al., 2002). Briefly, animals were anesthetized with the ketamine/xylazine mixture as above and placed into a standard stereotaxic apparatus. A 30 gauge stainless steel cannula was lowered 5.6 mm into the medial septum (+0.2 mm from bregma, 0.0 mm lateral), and animals received either Sap (0.22 μg) or vehicle [sterile saline (Sal)] in a total volume of 1.0 μl infused at a rate of 0.2 μl/min. The cannula was left in place for 5 min after each infusion. The cannula then was removed, the incision was sutured closed, and animals were placed onto a warm heating pad during recovery. All animals received analgesic (0.1 mg/kg buprenorphine) after surgery to alleviate pain. Fourteen to 16 d after infusion, animals were ovariectomized, and on the third day after surgery, half of each infusion group received a single injection of either E or O. Twenty-four hours after E or O injection, animals were killed for preparation of hippocampal slices.

Preparation and maintenance of hippocampal slices. On each recording day, three or four animals each from different treatment groups within a particular type of experiment (e.g., tamoxifen pretreatment or Sap lesion) were coded, and the code was not broken until all data analysis for those animals was complete. Rats were anesthetized with Nembutal (80 mg/kg) and transcardially perfused with ice-cold oxygenated (95% O_2/5% CO_2) artificial CSF (ACSF) containing (in mM): 125 NaCl, 25 NaHCO$_3$, 25 dextrose, 2.5 KCl, 1.25 NaH$_2$PO$_4$, 1 MgCl$_2$, 2 CaCl$_2$, pH 7.5. The brain was quickly removed and cooled in ice-cold oxygenated ACSF. For experiments with Sap- or Sal-infused animals, the rostral portion of each brain containing the medial septum was saved and frozen for later choline acetyltransferase (ChAT) immunohistochemistry. Using a Vibroslicer (Electron Microscopy Sciences, Fort Washington, PA), 300-μm-thick transverse hippocampal slices were cut into a bath of ice-cold oxygenated ACSF. Also, for Sap- or Sal-infused animals, slices interleaved with those used for electrophysiology were frozen for later analysis of ChAT activity. Slices for electrophysiology were transferred to a holding chamber where they remained submerged in oxygenated ACSF at 35°C for 30 min and then at room temperature (~24°C) until they were used for recording.

Electrophysiological recording. Slices were transferred to a recording chamber mounted on a Zeiss Axioskop (Oberkochen, Germany) where they were submerged in oxygenated ACSF maintained at 35 ± 1°C. Neurons in the slice were visualized using infrared differential interference videomicroscopy (Hamamatsu, Hamamatsu City, Japan). Somatic whole-cell current- or voltage-clamp recordings were obtained from CA1 pyramidal neurons using patch electrodes made from thick-walled borosilicate glass (Garner Glass, Claremont, CA) pulled on a P-97 micropipette puller (Sutter Instrument Co., Novato, CA) with an open tip resistance of 3–5 MΩ in ACSF. Series resistance (average 13 ± 4.7 MΩ) was compensated (70%), and a recording was terminated if a significant increase occurred. Data were collected with an Axopatch 200B amplifier (Axon Instruments, Foster City, CA) acquired and analyzed using Igor Pro software (WaveMetrics, Lake Oswego, OR).

Synaptically evoked action potentials were recorded in current clamp using a pipette solution containing (in mM): 115 K-gluconate, 20 KCl, 10 Na$_2$-creatinine phosphate, 20 HEPES, 2 EGTA, 2 MgATP, NaGTP, pH 7.3. Before recording, a cut in the slice was made between the CA1 and CA3 regions. A bipolar stimulating electrode was placed in the CA1 stratum radiatum ~200 μm lateral from the recorded cell soma halfway between the pyramidal cell layer and stratum lacunosum. Action potentials were evoked by increasing stimulus intensity in 1 μA steps delivered at a frequency of 0.1 Hz beginning from 40 μA until an action potential was triggered; all action potentials were overshooting. High-intensity stimuli (300 and 800 μA) were used to determine whether any cell fired multiple synaptically evoked action potentials. This stimulus–response paradigm was repeated three times for each cell, and the threshold stimulus current necessary to evoke an action potential was calculated for each cell.

Synaptically evoked IPSCs, spontaneous IPSCs, and mIPSCs were recorded in voltage clamp using a pipette solution containing (in mM): 140 CsCl, 2 MgCl$_2$, 10 HEPES, 2 EGTA, 2 MgATP, 0.3 NaGTP, 10 Na$_2$-creatinine phosphate, 0.1% biocytin, pH 7.2–7.3. The bath contained 5 mM kynurenic acid to block glutamate receptor-mediated synaptic transmission. To record synaptically evoked IPSCs, a stimulating electrode (patch pipette with chlorided silver wire) was placed in the CA1 pyramidal cell layer 50–100 μm away from the recording electrode. Stimulus–response curves were generated at a holding potential of −70 mV by varying stimulus intensity from the minimum current necessary to evoke a postsynaptic response to the current that produced a maximal response; stimuli were delivered at 0.1 Hz. Synaptically evoked IPSCs were blocked by the GABA$_A$ receptor antagonist bicuculline (10 μM). The stimulus–response protocol was repeated at least three times per cell, and the average of peak synaptically evoked IPSC amplitude at each stimulus intensity was calculated for each cell. Synaptically evoked IPSC rise and decay times were obtained from maximal currents, and data were averaged per cell. Paired-pulse depression of synaptically evoked IPSCs was measured using a stimulus intensity that evoked a maximal current. Pairs of IPSCs were evoked with interstimulus intervals from 10 to 300 msec delivered with 20 sec between stimulus pairs. The paired-pulse protocol was repeated at least three times per cell, and the ratio of IPSC amplitude evoked by the second pulse versus the first pulse (P2/P1) was calculated for each cell at each interstimulus interval. Stimulus–response curves were analyzed statistically with repeated-measures ANOVA. Synaptically evoked IPSC rise time and time to 50% decay were analyzed statistically with ANOVA followed by Turkey *post hoc* comparisons. Paired-pulse depression was analyzed statistically with repeated-measures ANOVA (for experiments with multiple interstimulus intervals) or ANOVA followed by Tukey *post hoc* comparisons (for experiments with a single interstimulus interval).

Spontaneous IPSCs were recorded from CA1 pyramidal cells without synaptic stimulation, and data were obtained from the first 500 spontaneous events per cell. Subsequently, 5 μM TTX was added to the bath to reveal mIPSCs from the same cell. Miniature IPSCs were recognized as events at least 2 SD above the amplitude of noise, as determined by recording in kynurenic acid and bicuculline. Data were collected from the first 500 mIPSCs per cell. The frequency, mean amplitude, and rise and decay time of TTX-sensitive (i.e., action potential-related) spontaneous IPSCs and mIPSCs were analyzed statistically using ANOVA followed by Tukey *post hoc* comparisons. Amplitude and decay time histograms for action potential-related spontaneous IPSCs and mIPSCs were analyzed statistically using the Kolmogorov–Smirnov test.

In some experiments, exogenous GABA was applied directly to the soma of a recorded cell using a PV830 pneumatic picopump (World Precision Instruments, Sarasota, FL). GABA application was repeated at least 10 times with a 1 min interval between applications, and measure-

ments of peak amplitude and decay time were averaged for each cell. The amplitude and time to 50% decay of GABA-evoked currents were analyzed statistically using Student's *t* test.

Immunohistochemistry for ChAT. ChAT immunohistochemistry was performed for each Sap- or Sal-infused animal to confirm cholinergic lesion in the Sap-infused animals. All tissue was coded, and the code was not broken until analysis of both immunohistochemical and enzyme activity assays for ChAT was complete. The rostral portion of each brain containing the medial septal area was fixed by immersion in 4% paraformaldehyde in 50 mM PBS for several hours and then in 4% paraformaldehyde in 15% sucrose at 4°C overnight. Brain tissue was coronally sectioned (40 μm) through the medial septal area using a freezing microtome. Sections were processed for immunohistochemical detection of ChAT as described previously (Gibbs, 1997).

Briefly, sections were incubated in the primary antiserum (1:3500; Chemicon International) for 72 hr at 4°C. After primary incubation, sections were rinsed thoroughly and incubated in biotinylated secondary antibody (1:250, anti-goat IgG; Vector Laboratories, Burlingame, CA). The sections were rinsed and incubated in avidin–biotin HRP complex (1:500; Vector Elite Kit) for 1 hr. Next, the tissue was incubated for 10 min in Tris acetate solution containing 3–3′-diaminobenzidine (0.5 mg/ml), H_2O_2 (0.01%), and $NiCl_2$ (0.032%). After the reaction, sections were rinsed, mounted onto subbed slides, dehydrated in graded ethanols, cleared in xylene, and coverslipped under DePex.

ChAT assay. Frozen, coded, hippocampal slices were thawed and dissociated by sonication in a medium containing EDTA (10 mM) and Triton X-100 (0.5%) and diluted to a concentration of 10 mg tissue per milliliter. An aliquot of each sample was used for the determination of total protein (Bradford, 1976). ChAT activity was measured as described previously (DeKosky et al., 1985).

Briefly, three 5 μl aliquots of each sample were incubated for 30 min at 37°C in a medium containing [^{3}H]acetyl-CoA (3.6 Ci/mmol, 30,000–40,000 dpm per tube, final concentration 0.25 mM acetyl CoA; Sigma, St. Louis, MO), choline chloride (10 mM), physostigmine sulfate (0.2 mM), NaCl (300 mM), sodium phosphate buffer, pH 7.4 (50 mM), and EDTA (10 mM). The reaction was terminated with 4 ml of sodium phosphate buffer (10 mM, pH 7.2) followed by the addition of 1.6 ml of acetonitrile containing 5 mg/ml tetraphenylboron. The amount of [^{3}H]acetylcholine produced was determined by adding 8 ml of EconoFluor scintillation mixture (Packard Instruments, Meriden, CT) and counting total counts per minute (cpm) in the organic phase using an LKB beta counter. Background was determined using identical tubes to which no sample was added. For each sample, the three reaction tubes containing sample were averaged, and the difference between total cpm and background cpm was used to estimate the total amount of acetylcholine produced per sample. ChAT activity was then calculated for each sample as picomoles of acetylcholine produced per hour per microgram of protein. All samples were assayed at the same time using the same stock of [^{3}H]acetyl-CoA, and the data were analyzed statistically using ANOVA followed by Tukey *post hoc* comparisons.

Results

Estrogen-induced disinhibition

Previously, we found that 24 hr of estrogen treatment significantly decreases the amplitude and prolongs the decay time of synaptically evoked IPSCs in CA1 pyramidal cells. Recordings of the mixed current (EPSC + IPSC) evoked by stimulation in the stratum radiatum suggested that these changes are associated with reduced disynaptic inhibition of CA1 pyramidal cells (Rudick and Woolley, 2001). To test directly whether 24 hr of estrogen treatment disinhibits CA1 pyramidal cells, we measured the stimulus current necessary to produce an action potential evoked by a stimulating electrode placed in the stratum radiatum. Current-clamp recordings were made with a K^+-gluconate internal solution. We found that estrogen significantly reduced the stimulus necessary to evoke an action potential, from 68.0 ± 2.97 μA in cells from oil-treated controls to 51.1 ± 2.84 in cells from
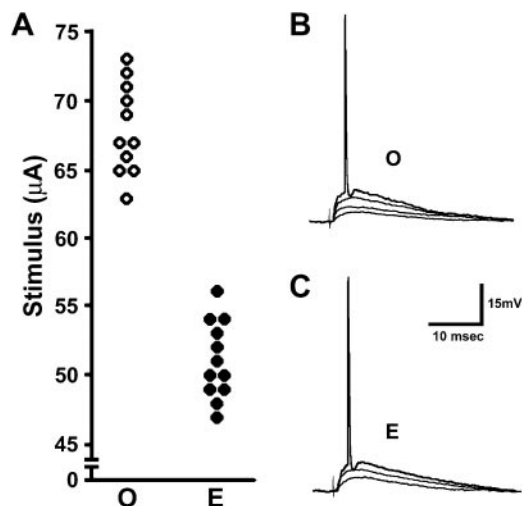

Figure 1. Estrogen treatment decreases the threshold for action potential firing in CA1 pyramidal cells. *A,* Plot of the minimum stimulus necessary to evoke an action potential in cells from oil-treated (O, open circles; *n* = 11 cells from 6 animals) and estrogen-treated (E, closed circles; *n* = 12 cells from 6 animals) groups. Action potential threshold was significantly lower for the cells in the estrogen-treated group (*p* < 0.01). *B,* Representative EPSPs and action potential from a cell in the O-treated group; stimuli for the traces shown were 40, 50, 60, and 70 μA (this cell first fired at 69 μA). *C,* Representative EPSPs and action potential from a cell in the E-treated group; stimuli for the traces shown were 40, 50, and 60 μA (this cell first fired at 51 μA).

estrogen-treated animals (*p* < 0.01) (Fig. 1). No cells in either group fired multiple action potentials, even at high stimulus intensities. The effect of estrogen to decrease action potential threshold was particularly robust in that the stimulus necessary to evoke an action potential in cells from oil-treated animals was greater than in cells from estrogen-treated animals in 100% of our experiments; there was no overlap between the data sets. We conclude from this result that 24 hr of estrogen treatment disinhibits CA1 pyramidal cells.

Effects of tamoxifen on estrogen-induced changes in synaptic inhibition

We used the selective estrogen receptor modulator tamoxifen to investigate whether the effects of estrogen on synaptic inhibition of CA1 pyramidal cells depend on an ER. In these experiments, we replicated both the estrogen-induced decrease in IPSC amplitude and prolongation of IPSC decay and found that each is completely blocked by pretreatment with tamoxifen. Tamoxifen is generally an ER antagonist in brain, but also can act as an ER agonist in some systems. To validate use of tamoxifen as an ER antagonist, we confirmed in a separate study that tamoxifen does not act as an ER agonist in CA1 (Rudick and Woolley, 2003). The advantage of tamoxifen for these studies is that unlike "pure" anti-estrogens, it readily crosses the blood–brain barrier. Although tamoxifen can block at least one rapid effect of estrogen (Rudick and Woolley, 2003), it fails to block many others (Morley et al., 1992; Aronica et al., 1994; Mermelstein et al., 1996; Watters and Dorsa, 1998), so inhibition by tamoxifen is a good indication of a classical ER-mediated mechanism.

Whole-cell voltage-clamp recordings were made using a CsCl-based internal solution and at a holding potential of −70 mV so that the $GABA_A$ receptor-mediated IPSC was an inward current. In the first series of experiments, synaptically evoked IPSCs recorded in cells from oil-treated or estrogen-treated animals that were pretreated either with vehicle (Fig. 2*A*,*B*, VO and VE) or with tamoxifen [TO or TE (Fig. 2*C*)] were used to generate
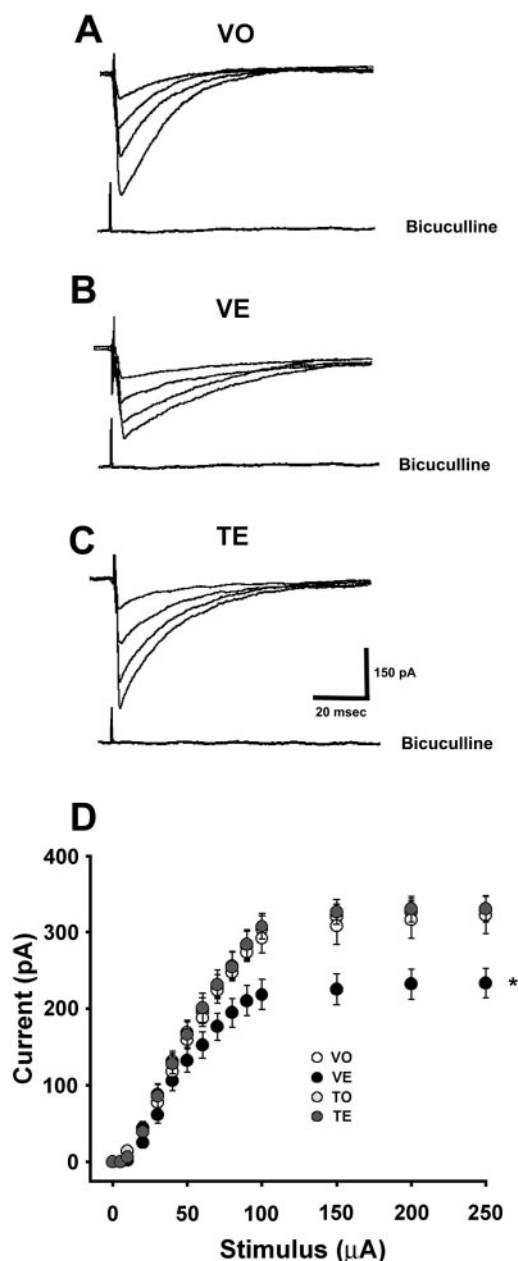
Figure 2. Tamoxifen blocks the estrogen-induced decrease in the amplitude of synaptically evoked IPSCs. All recordings were made with a CsCl-based internal solution at a holding potential of −70 mV so that GABA$_A$-mediated IPSCs are inward currents. *A*, Representative individual traces of IPSCs evoked in a VO cell using 30, 50, 100, and 250 μA stimulating current. *B*, Representative individual traces of IPSCs evoked in a VE cell using the same stimulus intensities as in *A*. *C*, Representative individual traces of IPSCs evoked in a TE cell using the same stimulus intensities as in *A*. Evoked currents are blocked by bicuculline. *D*, Averaged stimulus–response curves for VO (open circles; *n* = 12 cells from 6 animals), VE (black circles; *n* = 12 cells from 6 animals), TO (light gray circles; *n* = 11 cells from 6 animals), and TE (dark gray circles; *n* = 13 cells from 6 animals) groups. *Peak IPSC amplitude is significantly reduced in VE cells compared with TE, TO, and VO cells (*p* < 0.05).

Table 1. Kinetic parameters of synaptically evoked IPSCs

Treatment group	VO	VE	TO	TE
τ_{rise} (msec)	1.1 ± 0.2	1.2 ± 0.2	1.0 ± 0.1	0.9 ± 0.1
$\tau_{decay\ fast}$ (msec)	10.8 ± 1.3	15.7 ± 1.8*	10.6 ± 1.4	10.9 ± 1.6
$\tau_{decay\ slow}$ (msec)	29.7 ± 4.2	41.9 ± 4.7††	30.2 ± 4.1	32.3 ± 4.4
$\tau_{decay\ slow}$ relative amplitude (%)	40 ± 2.9	69 ± 4.3**	38 ± 2.7	42 ± 3.1
Time to 50% decay (msec)	14.1 ± 1.8	23.7 ± 3.1**	13.8 ± 1.7	13.3 ± 1.9

Data are mean ± SEM. Units are indicated in parentheses. Evoked IPSC rise time was not significantly different among groups. *Significant difference from TE, TO, and VO (*p* < 0.05). **Significant difference from TE, TO, and VO (*p* < 0.01). ††Significant difference from VO, TO (*p* < 0.01), and TE (*p* < 0.05).

in IPSC amplitude. Stimulus–response curves for VE cells were significantly different from those for VO, TO, or TE cells (*p* < 0.05), which were not different from each other (*p* > 0.1).

Estrogen also prolonged the decay time of evoked IPSCs. IPSC decay in CA1 pyramidal cells is best described by two time constants, $\tau_{decay\ fast}$ and $\tau_{decay\ slow}$ (Pearce, 1993; Rudick and Woolley, 2001), each of which was greater in VE compared with VO cells (all kinetics data are shown in Table 1). Additionally, the slower component of IPSC decay accounted for 69% of current in VE cells compared with only 40% in VO cells. For statistical comparison, we measured the time to 50% decay of IPSCs, which was significantly greater in VE than VO cells (*p* < 0.05). Pretreatment with tamoxifen itself did not affect the kinetics of evoked IPSCs (*p* > 0.1), but completely blocked the effects of estrogen on IPSC decay (*p* > 0.1). In contrast to IPSC decay time, the rise time of evoked IPSCs was unaffected by any treatment.

Previously, we demonstrated that the decrease in evoked IPSC amplitude was associated with a decrease in the frequency, but not amplitude, of TTX-insensitive mIPSCs recorded from the same cells (Rudick and Woolley, 2001). TTX-insensitive mIPSCs reflect spontaneous GABA release at individual synaptic sites; the frequency of mIPSCs is a functional measure of the number of GABAergic synapses, and mIPSC amplitude is a measure of the strength of individual GABAergic synapses. In the current study, we replicated the estrogen-induced decrease in mIPSC frequency and found that like the decrease in evoked IPSC amplitude, it is blocked by pretreatment with tamoxifen (Fig. 3). Miniature IPSC frequency was significantly lower in VE cells than in VO, TO (*p* < 0.01), or TE cells (*p* < 0.05), which were not different from each other (*p* > 0.1).

Analysis of histograms for mIPSC amplitude and decay time from cells in each treatment group provided additional information about estrogen-induced changes in GABAergic synapses and confirmed complete blockade of the effects of estrogen by tamoxifen. Miniature IPSC amplitude histograms (Fig. 4*A–C*) show that although estrogen does not significantly alter the mean amplitude of mIPSCs, it does produce a statistically significant skewing toward larger amplitude mIPSCs (Fig. 4*D*) (*p* < 0.01). This shift toward larger currents is clear evidence that the estrogen-induced decrease in evoked IPSC amplitude is not caused by a decrease in the strength of individual GABAergic synapses, because this would produce a shift in the direction of smaller mIPSCs. Additionally, comparison of mIPSC decay time histograms (Fig. 4*E–H*) revealed a subpopulation of mIPSCs with prolonged decay time in VE cells that parallels the longer decay of evoked IPSCs in the same animals; mIPSCs with prolonged decay also are evident in the VE traces shown in Figure 3*B*. Although group data are shown in Figure 4, it is important to note that mIPSC decay time histograms were clearly bimodal in 28 of the 32 individual cells from estrogen-treated animals in this study.
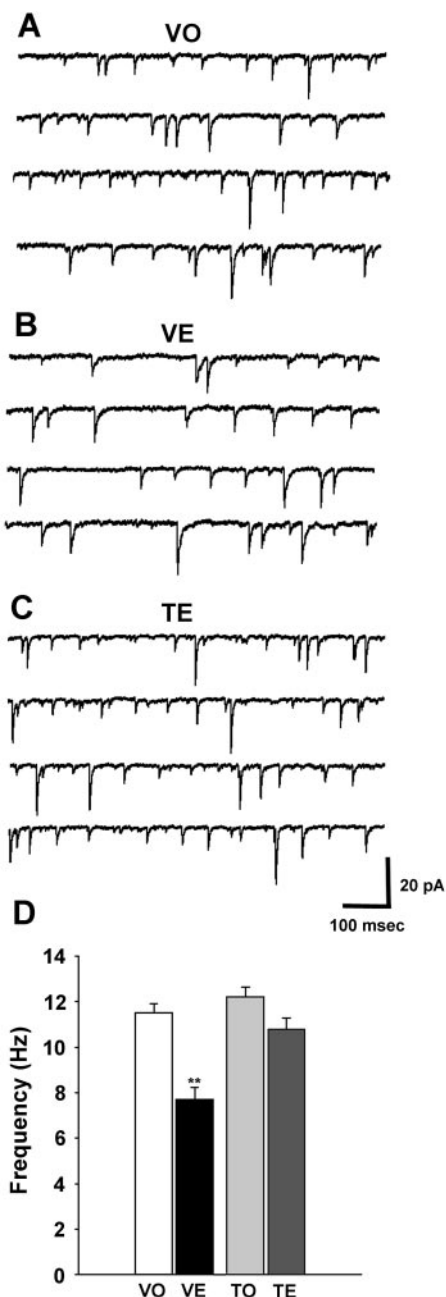
stimulus–response curves (Fig. 2*D*). Twenty-four hours of estrogen treatment had two principal effects on evoked IPSCs: decreased amplitude and increased decay time. Peak amplitude of evoked IPSCs was 30% lower in VE than VO cells (*p* < 0.05). Pretreatment with tamoxifen had no effect on evoked IPSC amplitude in oil-treated controls: stimulus–response curves were virtually identical for VO and TO cells (*p* > 0.1). However, tamoxifen pretreatment did block the estrogen-induced decrease

Figure 3. Tamoxifen blocks the estrogen-induced decrease in the frequency of TTX-insensitive mIPSCs. All recordings were made with a CsCl-based internal solution at a holding potential of −70 mV so that GABA$_A$-mediated mIPSCs are inward currents. *A–C*, Representative traces from four different VO cells (*A*), VE cells (*B*), and TE cells (*C*) showing mIPSCs. *D*, Bar graph of mean ± SEM frequency of mIPSCs in VO (open bars), VE (black bars), TO (light gray bars), and TE (dark gray bars) groups. Data were obtained from the first 500 mIPSCs from each of the same cells as in Figure 2*D*. **Significant difference from TO and VO (*p* < 0.01) and from TE (*p* < 0.05).

Pretreatment with tamoxifen did not affect the distributions of mIPSC amplitudes or decay times in control animals but completely blocked effects of estrogen on both measures. Miniature IPSC amplitude and decay time histograms for VE cells were significantly different from those for VO, TO, or TE cells (*p* < 0.01), which were not different from each other (*p* > 0.1). Together, these data demonstrate that estrogen acts through a tamoxifen-sensitive ER to regulate both disinhibition and prolongation of IPSCs in CA1 pyramidal cells.
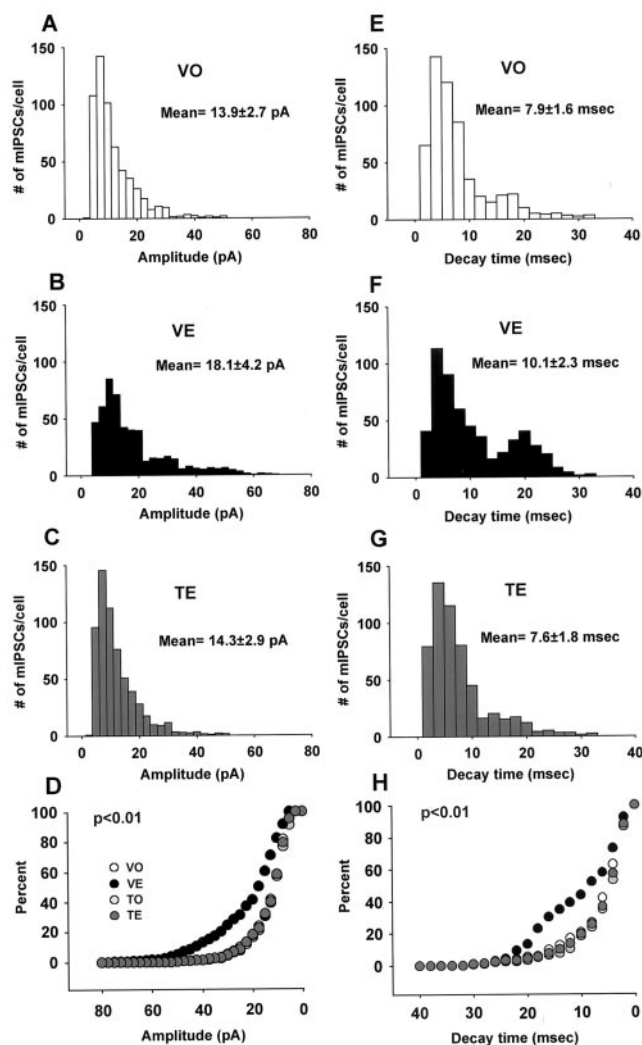

Figure 4. Tamoxifen blocks estrogen-induced changes in mIPSC amplitude and decay time distributions. *A–C*, mIPSC amplitude histograms for the VO group (*A*), VE group (*B*), and TE group (*C*). *D*, Cumulative histogram of mIPSC amplitudes for VO (open circles), VE (black circles), TO (light gray circles), and TE (dark gray circles). Mean mIPSC amplitude is not significantly affected by estrogen, but note the shift toward larger amplitude mIPSCs in the VE group (*p* < 0.01) that is absent in the TE group. *E–G*, mIPSC decay time histograms for the VO group (*E*), VE group (*F*), and TE group (*G*). *H*, Cumulative histogram of mIPSC decay times for VO (open circles), VE (black circles), TO (light gray circles), and TE (dark gray circles). Mean mIPSC decay time is not significantly affected by estrogen, but note the subpopulation of longer decay time mIPSCs in the VE group (*p* < 0.01) that is absent in the TE group. Data were obtained from the same 500 mIPSCs per cell as in Figure 3*D*.

Paired-pulse depression and GABA-evoked currents

The decreases in evoked IPSC amplitude and mIPSC frequency in cells from estrogen-treated animals suggest that estrogen may decrease probability of release at GABAergic synapses. To investigate this possibility, we measured paired-pulse depression of evoked IPSCs (Fig. 5*A*), which is an indicator of probability of release. We found that paired-pulse depression was significantly reduced in cells from estrogen- versus oil-treated animals (*p* < 0.05); the difference was greatest with interstimulus intervals of ≤100 msec (Fig. 5*B*). For example, with a 50 msec interstimulus interval, the P2/P1 ratio in controls cells was 0.67 ± 0.05, indicating 33% depression of the second response, whereas P2/P1 was 0.95 ± 0.02 in cells from estrogen-treated animals, indicating only 5% depression. These data suggest that the decrease in evoked IPSC amplitude and mIPSC frequency induced by estro-
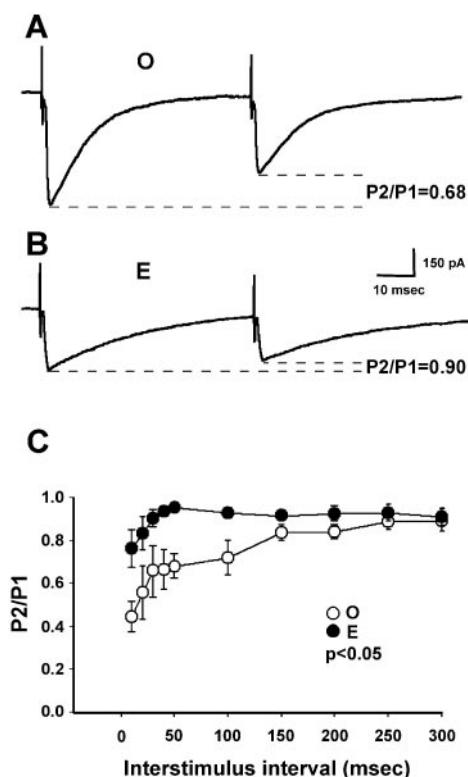
Figure 5. Estrogen decreases paired-pulse depression of evoked IPSCs in CA1 pyramidal cells. Recordings were made with a CsCl-based internal solution at a holding potential of −70 mV so that GABA$_A$-mediated spontaneous IPSCs are inward currents. *A, B*, Representative traces of pairs of IPSCs from an O-treated cell (*A*) and an E-treated cell (*B*) evoked with a 50 msec interstimulus interval. *C*, Plot of P2/P1 ratios in the O-treated group (open circles; *n* = 11 cells from 6 animals) compared with the E-treated group (black circles; *n* = 13 cells from 6 animals). Note that P2/P1 is closer to 1.0 in cells from the E-treated group, indicating less paired-pulse depression (*p* < 0.05).

gen is caused, at least in part, by a functional change in GABAergic synapses that decreases the probability of GABA release. However, other factors such as receptor desensitization also may influence measures of paired-pulse depression.

To evaluate the effect of estrogen treatment on postsynaptic and extrasynaptic GABA receptors, we measured the current evoked by application of GABA to the soma using a picopump (e.g., 1 sec application of 500 μM GABA). Experiments with exogenous GABA application revealed no differences in the amplitude or kinetics of GABA-evoked currents in cells from oil- (*n* = 8) and estrogen-treated (*n* = 9) animals (*p* > 0.1 on all measures; data not shown). These data indicate that estrogen does not produce a global (i.e., postsynaptic and extrasynaptic) increase in the decay time of GABA-evoked currents, but rather increases decay time of currents selectively at a subset of GABAergic synapses. This observation is consistent with the mIPSC decay time histograms, which show that only a subset of mIPSCs is prolonged in cells from estrogen-treated animals. However, because synaptic receptors may be only a fraction of those activated by exogenous GABA application, it is not possible to conclude from this negative result whether the effect of estrogen on IPSC decay time is presynaptic or postsynaptic.

Effects of cholinergic lesions on estrogen-induced changes in synaptic inhibition

Our results with tamoxifen indicated than an ER is involved in mediating the effects of estrogen on synaptic inhibition of CA1

pyramidal cells. As mentioned previously, nuclear ER-α is not expressed in pyramidal cells but is expressed in a small subset of GABAergic neurons (in dorsal CA1, where all our recordings were made) (Hart et al., 2001). Additionally, Hart et al. (2001) found no evidence for ER-β expression in the adult hippocampus. Only ~10% of GABAergic neurons located within the pyramidal cell layer, i.e., those most likely to be immediately presynaptic to pyramidal cell bodies, express ER-α. Although the small number of ER-expressing GABA neurons in the hippocampus may participate in estrogen-induced changes in inhibition of CA1 pyramidal cells, an additional possibility is that ER-expressing cells in hippocampal afferents also play a critical role.

Several lines of evidence point to basal forebrain cholinergic neurons as likely candidates for mediating the effects of estrogen in the hippocampus. First, ~37% of cholinergic neurons in the medial septum bind estrogen and express ER-α (Shughrue et al., 2000). Second, estrogen enhances septohippocampal cholinergic neurotransmission as reflected by increases in medial septal ChAT mRNA, protein (Gibbs, 1996, 1997), and activity (Luine 1985), as well as high-affinity choline uptake (Gibbs, 2000) and acetylcholine release (Gibbs et al., 1997) in the hippocampus. Although acetylcholine influences neuronal activity through both ionotropic nicotinic and metabotropic muscarinic acetylcholine receptors, a recent study demonstrated that M2 muscarinic receptors are required for estrogen-induced changes in NMDA receptor binding in CA1 (Daniel and Dohanich, 2001).

To explore the possibility that basal forebrain cholinergic neurons are involved in estrogen-induced changes in synaptic inhibition of hippocampal neurons, we tested the ability of estrogen to disinhibit CA1 pyramidal cells in animals in which basal forebrain cholinergic neurons had been eliminated by previous infusion of 192IgG-Sap into the medial septum. For each animal in this study, we confirmed the effectiveness of Sap infusion on the basis of ChAT immunoreactivity in the basal forebrain and ChAT activity in hippocampal slices interleaved with those used for electrophysiology. These analyses showed that intraseptal infusions of Sap resulted in a substantial loss of ChAT-positive cells in the medial septum and diagonal band of Broca (Fig. 6A–C) and significantly decreased ChAT activity in the hippocampus by 85% (*p* < 0.01) (Fig. 6D).

Electrophysiological analysis demonstrated that the ability of estrogen to disinhibit CA1 pyramidal cells was significantly attenuated in Sap-lesioned animals, but it was not completely blocked. As before, we evaluated evoked IPSCs and mIPSCs. Removal of basal forebrain cholinergic neurons by itself had no effect on measures of synaptic inhibition in CA1; data from Sap-O and Sal-O animals were indistinguishable (*p* > 0.1 on all measures). As expected from previous experiments, estrogen decreased the peak amplitude of synaptically evoked IPSCs in Sal-infused animals by 35% (Fig. 7A) (*p* < 0.05). In Sap-lesioned animals, however, the estrogen-induced decrease in evoked IPSC amplitude was significantly attenuated in that peak IPSC amplitude was reduced by only 13% and was significantly different from all other groups (*p* < 0.05) (Fig. 7A). The effect of estrogen on paired-pulse depression of IPSCs also was reduced by Sap lesion (Fig. 7B). In Sal-infused controls, the P2/P1 ratio with a 50 msec interstimulus interval was 0.63 ± 0.05 Sal-O cells and 0.93 ± 0.06 Sal-E cells (*p* < 0.01), whereas in Sap-lesioned animals, estrogen did not significantly alter the P2/P1 ratio (0.64 ± 0.04 in Sap-O vs 0.72 ± 0.06 in Sap-E; *p* = 0.054). Similar to evoked IPSC amplitude, the frequency of mIPSCs in Sap-E animals was intermediate between Sal-E animals and Sal-O and Sap-O animals (*p* < 0.05; Sap-E vs all other groups) (Fig. 7C). Additionally, the skewing of
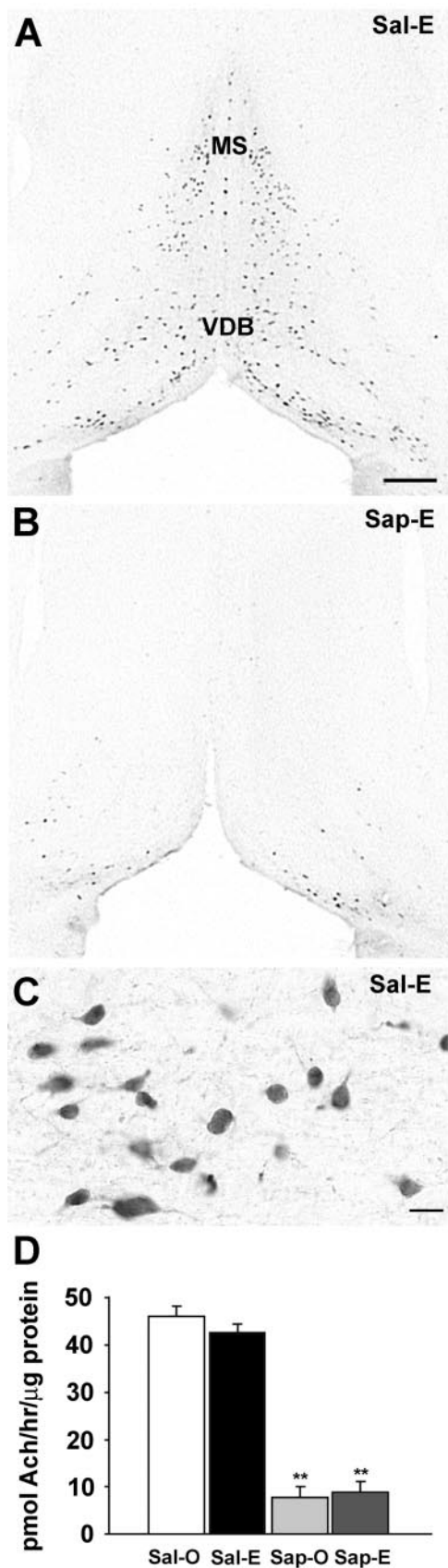
Figure 6. Infusion of 192IgG-saporin into the medial septum substantially reduces the number of cholinergic neurons in the basal forebrain and decreases ChAT activity in the hippocampus. A–C, Photomicrographs of ChAT-immunolabeled cells in Sal- and Sap-infused animals. Low magnification view of ChAT-labeled cells in a Sal-E control (A) and a Sap-E (B) animal.
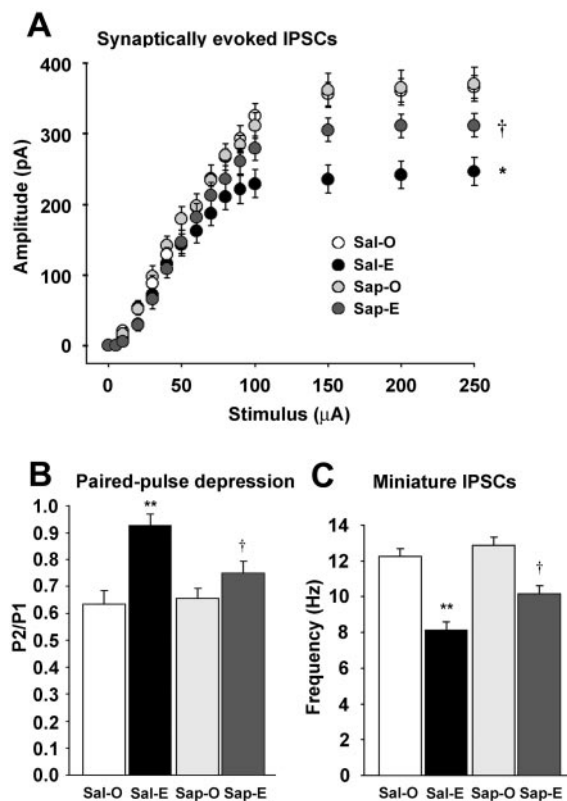

Figure 7. 192IgG-saporin lesion significantly attenuates estrogen-induced disinhibition but does not completely block it. A, Averaged stimulus–response curves for synaptically evoked IPSCs in Sal-O (open circles; $n = 12$ cells from 6 animals), Sal-E (black circles; $n = 12$ cells from 6 animals), Sap-O (light gray circles; $n = 9$ cells from 6 animals), and Sap-E (dark gray circles; $n = 8$ cells from 6 animals) groups. B, Bar graph of mean $\pm$ SEM. P2/P1 ratio for evoked IPSCs in Sal-O, Sal-E, Sap-O, and Sap-E groups (50 msec interstimulus interval). Note that P2/P1 in the Sal-E group is closer to 1.0 than in other groups, indicating less paired-pulse depression in Sal-E. C, Bar graph of mean $\pm$ SEM frequency of mIPSCs for Sal-O, Sal-E, Sap-O, and Sap-E groups. *Significant difference from Sal-O, Sap-O, and Sap-E ($p < 0.05$); **significant difference from Sal-O and Sal-O ($p < 0.01$); †significant difference from Sal-O, Sap-O, and Sal-E ($p < 0.05$; trend from Sap-O in B, $p = 0.054$).

mIPSC amplitudes toward larger currents was intermediate in Sap-E animals (data not shown). With the exception of paired-pulse experiments in which estrogen did not have a statistically significant effect in Sap-lesioned animals, data from the Sap-E cells were significantly different from cells in all other groups ($p < 0.05$). These results demonstrate that the basal forebrain cholinergic system plays a critical role in estrogen-induced disinhibition of hippocampal CA1 pyramidal cells. The observation that Sap lesion produced only a partial blockade of the effects of estrogen indicates that in addition to basal forebrain cholinergic neurons, other cells also are likely to be involved in estrogen-induced disinhibition in the hippocampus.

Although we expected that cholinergic tone in an acute hip-

←

Note the significant reduction in ChAT labeling in the medial septum (MS) and vertical diagonal band (VDB) in Sap-E compared with Sal-E. C, High magnification view of ChAT-labeled cells in a Sal-E control. Scale bars: (in A) A, B, 400 μm; C, 50 μm. D, Bar graph of mean $\pm$ SEM. ChAT activity in hippocampal slices interleaved with those used for electrophysiology demonstrating effective reduction of cholinergic activity: Sal-O (open bars; $n = 12$ slices from 6 animals), Sal-E (black bars; $n = 12$ slices from 6 animals), Sap-O (light gray bars; $n = 9$ slices from 6 animals), and Sap-E (dark gray bars; $n = 8$ slices from 6 animals) groups. **Significant difference from Sal-O and Sal-E ($p < 0.01$).
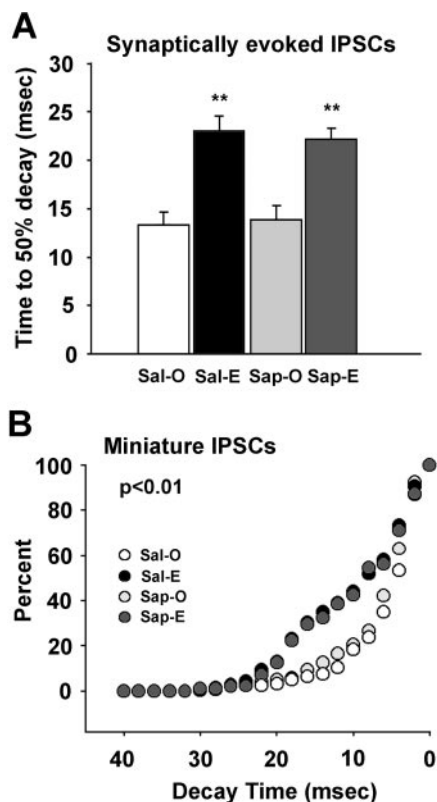
Figure 8. 192IgG-saporin lesion has no effect on estrogen-induced prolongation of IPSC decay times. *A*, Bar graph of mean ± SEM decay times of synaptically evoked IPSCs in Sal-O (open bars), Sal-E (black bars), Sap-O (light gray bars), and Sap-E (dark gray bars) groups. *B*, Cumulative histogram of mIPSC decay time distributions for Sal-O (open circles), Sal-E (black circles), Sap-O (light gray circles), and Sap-E (dark gray circles). Note the leftward shift in mIPSC decay time in both the Sal-E and Sap-E groups ($p < 0.01$) that is not observed in the Sal-O and Sap-O groups. Data are from the same cells as in Figure 6. **Significant difference from oil-treated groups ($p < 0.01$).

Table 2. Kinetic parameters of synaptically evoked IPSCs

Treatment group	Sal-O	Sal-E	Sap-O	Sap-E
τ_{rise} (msec)	1.0 ± 0.2	1.2 ± 0.3	0.9 ± 0.1	1.1 ± 0.2
$\tau_{decay\ fast}$ (msec)	10.9 ± 1.3	$15.5 \pm 1.7*$	11.1 ± 1.4	$15.3 \pm 1.6*$
$\tau_{decay\ slow}$ (msec)	28.8 ± 4.8	$42.0 \pm 5.0**$	30.5 ± 4.7	$41.1 \pm 4.5*$
$\tau_{decay\ slow}$ relative amplitude (%)	37 ± 2.5	$68 \pm 4.4**$	39 ± 2.8	$66 \pm 4.2**$

Data are mean ± SEM. Units are indicated in parentheses. Evoked IPSC rise time was not significantly different between groups. *Significant difference from the corresponding oil control ($p < 0.05$). **Significant difference from the corresponding oil control ($p < 0.01$). Figure 7A shows time to 50% decay from these animals.

forms multiple inhibitory synapses with each pyramidal cell that it contacts (Buhl et al., 1994; Freund and Buzsaki, 1996). Given this circuitry, we considered the possibility that estrogen might selectively influence a subset of the GABAergic neurons that innervate an individual CA1 pyramidal cell. To test this idea, we recorded TTX-sensitive spontaneous IPSCs, which reflect GABA released by action potential firing in inhibitory neurons. We obtained action potential-related spontaneous IPSCs by recording all spontaneous IPSC events (i.e., mIPSCs and spontaneous IPSCs attributable to inhibitory neuron firing) first in normal ACSF and then after addition of TTX to the bath (i.e., mIPSCs only). For each cell, amplitude histograms were plotted before (Fig. 9*A,B*, insets) and after TTX, and the distribution of events remaining after TTX was subtracted from the distribution of all events to reveal TTX-sensitive spontaneous IPSCs (326 ± 75 per cell). These action potential-related spontaneous IPSCs (referred to hereafter as spontaneous IPSCs) were collected from cells in animals treated only with oil or estrogen, as well as in oil- and estrogen-treated animals in the Sap-lesion study. Data from non-infused and Sal-infused animals were indistinguishable, so only data from Sal- and Sap-infused animals are shown.

Analysis of spontaneous IPSCs indicated that estrogen does not alter the number of inhibitory neurons in functional synaptic contact with CA1 pyramidal cells but that the current produced by each inhibitory neuron action potential, on average, is reduced. Similar to the effect of estrogen on evoked IPSC amplitude, estrogen treatment significantly decreased the mean amplitude of spontaneous IPSCs by 30% in cells from Sal-infused animals (Fig. 9*C*) ($p < 0.05$). As was the case with other measures of inhibition, Sap-lesion itself had no effect on the amplitude of spontaneous IPSCs in oil-treated controls ($p > 0.10$). Additionally, estrogen did not significantly alter the amplitude of spontaneous IPSCs in Sap-lesioned animals ($p = 0.09$ vs Sap-E vs Sap-O), although mean amplitude was slightly lower (by 9%) (Fig. 9*C*). Importantly, in contrast to the effect of estrogen on the amplitude of spontaneous IPSCs, estrogen had no effect on spontaneous IPSC frequency (Fig. 9*D*) ($p > 0.10$), nor was spontaneous IPSC frequency affected by the Sap lesion itself (Fig. 9*D*). Together, our spontaneous IPSC amplitude and frequency data are consistent with an estrogen-induced decrease in probability of GABA release that is distributed across multiple presynaptic neurons in contact with an individual CA1 pyramidal cell. Our results do not support the suggestion that estrogen substantially decreases probability of release at synapses from a subset of presynaptic inhibitory neurons, because this would be expected to decrease the frequency of spontaneous IPSCs. Interestingly, the lack of an effect of Sap lesion itself on spontaneous IPSC amplitude or frequency indicates that altering cholinergic tone in the hippocampus *in vivo* does not have a lasting effect on tonic inhibition of pyramidal cells, i.e., that is evident in a hippocampal slice.

Analysis of spontaneous IPSC decay times indicated that

pocampal slice, i.e., denervated from subcortical inputs, would be minimal, we performed additional experiments to confirm that the effects of estrogen on synaptic inhibition are not caused by an enhancement of presynaptic cholinergic function in the slice. We recorded paired-pulse depression and mIPSC frequency in cells from nonlesioned oil- ($n = 6$) and estrogen-treated ($n = 4$) animals before and after bath application of the nonselective muscarinic receptor antagonist atropine (1–5 μM) and found that neither measure was affected by atropine ($p > 0.1$; data not shown). These data indicate that estrogen-induced disinhibition in CA1 is not caused by a difference in cholinergic activity in the slice 24 hr after estrogen treatment.

Interestingly, in contrast to the effect of Sap lesion on estrogen-induced disinhibition, the ability of estrogen to prolong IPSC decay times was unaffected by elimination of basal forebrain cholinergic neurons. Synaptically evoked IPSCs were similarly prolonged in Sal-E and Sap-E cells (Fig. 8*A*, Table 2), and the subpopulation of prolonged mIPSCs was similarly present in Sal-E and Sap-E cells (Fig. 8*B*). Thus, analysis of Sap-lesioned animals demonstrated that the effects of estrogen on IPSC amplitudes versus decay times are separable, indicating that different mechanisms mediate these two effects of estrogen on synaptic inhibition of hippocampal CA1 pyramidal cells.

Action potential-related spontaneous IPSCs

Each CA1 pyramidal cell receives inhibitory synaptic input from multiple GABAergic neurons, and each GABAergic neuron
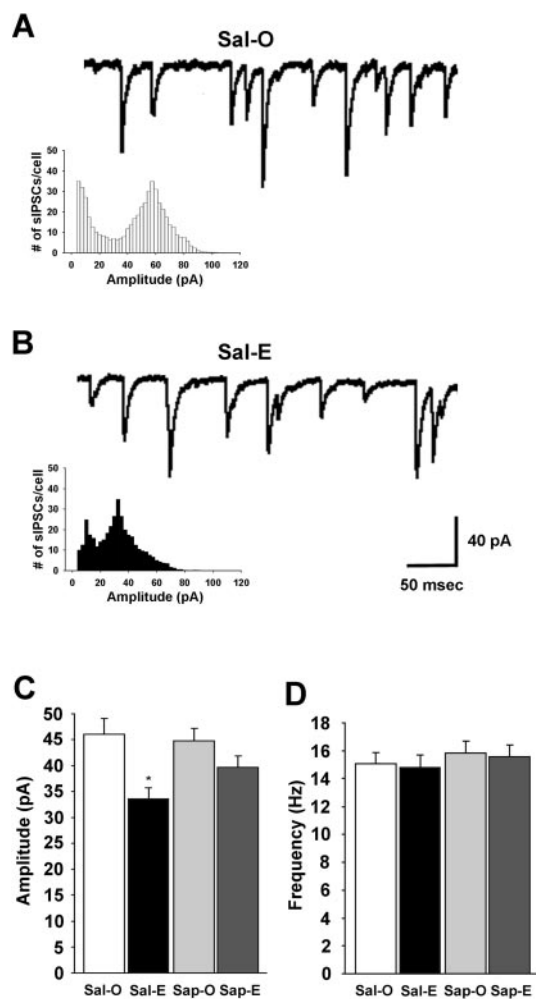
Figure 9. Estrogen decreases the amplitude, but not frequency, of action potential-related spontaneous IPSCs, and this decrease is blocked by 192IgG-saporin lesion. Recordings were made with a CsCl-based internal solution at a holding potential of −70 mV so that GABA$_A$-mediated spontaneous IPSCs are inward currents. A, B, Representative traces of spontaneous IPSC events (mIPSCs and action potential-related IPSCs) from a Sal-O cell (A) and a Sal-E cell (B). Insets, Amplitude histograms for all spontaneous IPSC events in each group; note two peaks, corresponding to mIPSCs and action potential-related IPSCs. C, Bar graph of the mean ± SEM amplitude of action potential-related (i.e., TTX-sensitive) spontaneous IPSCs in Sal-O, Sal-E, Sap-O, and Sap-E groups. Note the estrogen-induced decrease in action potential-related spontaneous IPSC amplitude in Sal animals ($p < 0.05$) but not Sap animals ($p = 0.09$; Sap-E vs Sap-O). D, Bar graph of the mean ± SEM frequency of action potential-related spontaneous IPSCs in Sal-O, Sal-E, Sap-O, and Sap-E groups. Neither estrogen nor 192IgG-saporin lesion affects the frequency of these events. Data were collected from 326 ± 75 action potential-related spontaneous IPSCs in the same cells as in Figure 6. *Significant difference from Sal-O, Sap-O ($p < 0.05$).

Figure 10. Estrogen increases the decay time of action potential-related spontaneous IPSCs, but this increase is unaffected by 192IgG-saporin lesion. A, Bar graph of mean ± SEM decay time of action potential-related spontaneous IPSCs in Sal-O, Sal-E, Sap-O, and Sap-E groups. B, C, Decay time histograms for action potential-related spontaneous IPSCs in the Sal-O group (B) and Sal-E group (C). Note that mean decay time of action potential-related spontaneous IPSCs is significantly increased by estrogen and that the distribution of action potential-related spontaneous IPSC decay times is unimodal but broader and shifted toward prolonged currents in the Sal-E-treated cells ($p < 0.05$). *Significant difference from the O-treated groups ($p < 0.05$). Data are from the same action potential-related spontaneous IPSCs as in Figure 9, C and D.

estrogen-induced prolongation of IPSCs also appears to be an effect that is distributed across presynaptic GABA neurons and not an effect on synapses formed by a subset of GABA neurons. One possibility suggested by analysis of mIPSC decay time histograms is that fast versus slow decay time mIPSCs might arise from distinct subsets of presynaptic inhibitory neurons. If this were the case, one would expect decay time histograms for action potential-related spontaneous IPSCs to be bimodal, similar to those for mIPSCs. Alternatively, if individual inhibitory neurons form a mixture of synapses with fast versus slow decay times, this would result in a unimodal decay time histogram for spontaneous IPSCs. Our findings point to the second possibility. First, consistent with the prolonged 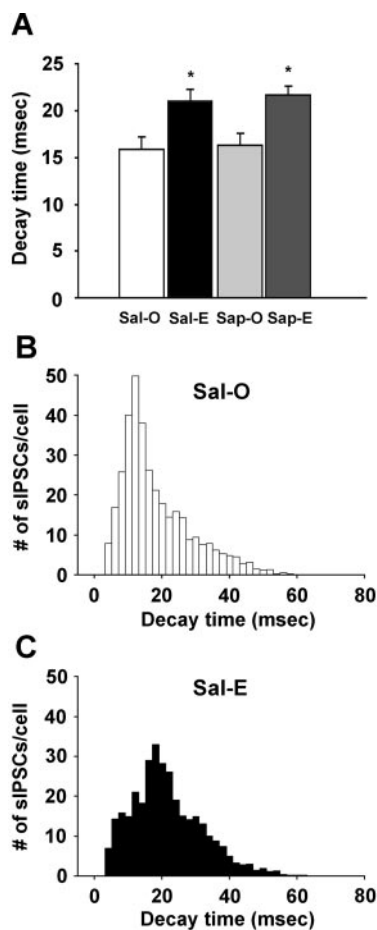decay time of evoked IPSCs, mean decay time of spontaneous IPSCs was significantly greater in cells from Sal-infused, estrogen-treated animals compared with cells from oil-treated controls ($p < 0.05$) (Fig. 10A). Second, in contrast to the bimodal decay time histograms for mIPSCs from estrogen-treated animals, decay time histograms for spontaneous IPSCs in cells from estrogen-treated animals were unimodal in all cells recorded, but the distribution was broader and shifted toward prolonged decay times (Fig. 10C) compared with controls (Fig. 10B). These data suggest that individual inhibitory neurons form a mixture of synapses with fast versus slow decay times, which in concert produce a relatively prolonged IPSC in estrogen-treated animals. Also consistent with data from evoked IPSCs, Sap lesion had no effect on spontaneous IPSC decay time or the estrogen-induced increase in spontaneous IPSC decay time (Fig. 10A).

Discussion

Our results provide five novel insights into the mechanism by which estrogen regulates synaptic inhibition of hippocampal CA1 pyramidal cells. (1) The effects of estrogen on pyramidal cell IPSCs result in disinhibition of these cells; (2) estrogen regulation

of synaptic inhibition, both disinhibition and prolongation of IPSCs, is entirely dependent on a tamoxifen-sensitive ER; (3) estrogen-induced disinhibition is partially dependent on basal forebrain cholinergic neurons, whereas the prolongation of IPSCs is not at all dependent on these cells; (4) estrogen-induced disinhibition appears to involve a decrease in the probability of transmitter release at GABAergic synapses; and (5) estrogen-induced disinhibition is associated with a decrease in the synaptic current produced by action potentials in individual inhibitory neurons rather than a decrease in the number of inhibitory neurons in functional contact with each CA1 pyramidal cell. Because estrogen-induced changes in synaptic inhibition precede and are likely to be causally related to enhancement of excitatory synaptic structure and function in the hippocampus, these findings contribute to understanding the chain of events by which estrogen influences hippocampal circuitry.

Estrogen-induced disinhibition
CA1 pyramidal cells are innervated by multiple GABAergic neurons, and each presynaptic GABA neuron forms multiple inhibitory synapses with individual postsynaptic pyramidal cells (Buhl et al., 1994; Freund and Buzsaki, 1996). Our recordings of paired-pulse depression and action potential-related spontaneous IPSCs indicate that estrogen-induced disinhibition is associated with a decrease in probability of GABA release and a reduction in the amplitude of IPSCs produced by action potentials in individual inhibitory neurons. Currently it is not known whether the decrease in probability of release is distributed similarly across the multiple GABAergic synapses formed by an individual presynaptic neuron or whether the decrease in release probability may be unequally distributed within an individual presynaptic neuron, resulting in functional silencing of a subset of GABA synapses formed by an individual presynaptic cell. Interestingly, observations in the arcuate nucleus of the hypothalamus provide a precedent for the second possibility. Twenty-four hours of estrogen exposure induces a physical retraction of some axosomatic GABAergic inputs to neurons in the arcuate (Parducz et al., 1993), silencing those synapses and disinhibiting arcuate neurons (Parducz et al., 2002). The possibility that estrogen functionally silences a subset of GABAergic synapses on CA1 pyramidal cells is particularly interesting because it suggests that individual synapses arising from the same presynaptic neuron are regulated differentially.

ER requirement for estrogen-induced disinhibition
We found that estrogen-induced disinhibition of CA1 pyramidal cells is blocked completely by pretreatment with tamoxifen, indicating estrogen action through an ER. Estrogen could regulate synaptic inhibition of CA1 pyramidal cells by acting directly on ER-expressing cells within the hippocampus and/or by acting on ER-expressing cells in brain regions that project to the hippocampus, such as the medial septum in the basal forebrain.

We used 192IgG-saporin infusion into the medial septum to test the possibility that basal forebrain cholinergic neurons are critically involved in estrogen-induced disinhibition of hippocampal CA1 pyramidal cells. As described earlier, the suggestion that estrogen acts directly within basal forebrain nuclei such as the medial septum to regulate changes in hippocampal function is supported by the observations that cholinergic neurons in the medial septum express ER-α (Shughrue et al., 2000), and some of the effects of estrogen on excitatory synapses in CA1 depend on cholinergic activity, particularly mediated by the M2 muscarinic receptor (Daniel and Dohanich, 2001). We found

that estrogen-induced disinhibition of hippocampal neurons was significantly attenuated in saporin-lesioned animals, demonstrating a role for the basal forebrain cholinergic system, but it was not blocked completely. There are at least two explanations for the partial effect of saporin lesion. Estrogen may act in two separate locations, for example within the basal forebrain and the hippocampus, in parallel to disinhibit CA1 pyramidal cells. Alternatively, it is possible that cholinergic deafferentation increases the sensitivity of hippocampal neurons to residual cholinergic input, which could support some degree of estrogen-induced disinhibition.

The distribution of ER-expressing cells within the hippocampus suggests that estrogen also could act directly on a subset of hippocampal GABA neurons to regulate inhibition of CA1 pyramidal cells. Although pyramidal cells in CA1 do not express classical ERs, nuclear ER-α is concentrated in a subset of GABAergic neurons at the border between the stratum radiatum and lacunosum-moleculare (Hart et al., 2001). Interestingly, some border neurons inhibit other inhibitory neurons that then inhibit CA1 pyramidal cells (Kunkel et al., 1988; Lacaille and Schwartzkroin, 1988) and thus could mediate disinhibition of pyramidal cells through intermediate GABA neurons. Because border neurons project to multiple other GABA neurons, and GABA neurons each innervate 1000 or more pyramidal cells (Freund and Buzsaki, 1996), this interaction provides a way that estrogen action on a small number of border neurons could be multiplicatively amplified to affect many CA1 pyramidal cells.

Models of estrogen-induced disinhibition involving the basal forebrain
The hippocampus receives both GABAergic and cholinergic input from basal forebrain regions such as the medial septum (Paxinos, 1995), either of which could play a role in estrogen-induced disinhibition of CA1 pyramidal cells. One possibility is that estrogen stimulates cholinergic neurons in the medial septum that project locally to septohippocampal GABAergic neurons (Brauer et al., 1998). Acetylcholine released in the septum provides a strong excitatory drive to the GABA neurons in the septohippocampal pathway (Alreja et al., 2000). The GABAergic component of the septohippocampal pathway targets GABAergic neurons in the hippocampus and thereby can regulate inhibition of hippocampal pyramidal cells (Freund and Antal, 1988). Given this circuitry, an estrogen-induced increase in cholinergic stimulation of GABAergic projection cells could produce disinhibition of hippocampal pyramidal cells. Because this model suggests estrogen regulation of inhibition at the level of entire hippocampal GABA neurons, it is more consistent with an effect of estrogen to decrease probability of release that is distributed similarly across the multiple GABAergic synapses formed by an individual inhibitory neuron.

A second possibility is that estrogen acts directly on cholinergic septohippocampal projection neurons to increase acetylcholine release (Gibbs et al., 1997) and thereby influences a subset of hippocampal GABAergic synapses that is sensitive to cholinergic modulation. The ability of an M2 muscarinic antagonist to block the effects of estrogen on NMDA receptor binding in CA1 (Daniel and Dohanich, 2001) suggests involvement of M2 receptors in such a scenario. Interestingly, only a subset of the parvalbumin-expressing inhibitory axonal varicosities in the CA1 pyramidal cell layer co-label for the M2 receptor (Hajos et al., 1998), suggesting that a only subset of synapses from an individual inhibitory neuron may be responsive to acetylcholine via M2 receptors. Because this model includes differential sensitivity

of individual GABA synapses to acetylcholine, it suggests an estrogen-induced decrease in probability of release that is unevenly distributed, possibly leading to functional silencing of a subset of GABA synapses formed by an individual inhibitory neuron. Additionally, it is important to note that however the estrogen–basal forebrain interaction works to disinhibit CA1 pyramidal cells, there must be a way that the effect of estrogen *in vivo* is translated into longer-lasting disinhibition that can be detected in a hippocampal slice 24 hr after estrogen and in the absence of septal input.

Several alternatives to the models discussed above also exist. For example, although our data indicate that basal forebrain cholinergic neurons are involved in estrogen-induced disinhibition, they do not distinguish between a direct effect of estrogen on these cells and the possibility that basal forebrain cholinergic neurons play a permissive role in estrogen-induced disinhibition. Some noncholinergic neurons in the medial septum also express ER-α (Shughrue et al., 2000), and cholinergic cells may regulate their activity. Additionally, although our tamoxifen data demonstrate ER involvement in estrogen-induced disinhibition, this may occur through a classical or nonclassical mechanism. Milner et al. (2001) reported that a small percentage of axonal varicosities in the CA1 pyramidal cell layer (i.e., likely GABAergic) express ER-α, suggesting the possibility that estrogen influences some GABAergic synapses directly.

Estrogen action on IPSC decay time

We found that tamoxifen completely blocked the effect of estrogen to prolong IPSC decay time, indicating action through an ER, whereas elimination of basal forebrain cholinergic neurons had no effect on estrogen-induced prolongation of IPSCs. Estrogen does not appear to alter GABA receptor kinetics globally, as evidenced by no effect on GABA-evoked currents. Recordings of both GABA-evoked currents and mIPSCs suggest that estrogen acts to prolong currents specifically at a subset of GABAergic synapses.

The prolongation of IPSC decay time could occur through postsynaptic changes in the subunit composition of GABA$_A$ receptors and/or changes in GABA transporter function, which could affect GABA uptake from the synaptic cleft. Precedents exist for each possibility. For example, regulation of the $\alpha1$ and $\alpha2$ (Hollrigel and Soltesz, 1997; Lavoie et al., 1997) or $\alpha4$ (Smith et al., 1998) GABA$_A$ receptor subunits has been shown to alter IPSC decay time. Additionally, regulation of the GAT-1 GABA transporter also can alter the decay time of IPSCs (Thompson and Gahwiler, 1992). Although studies of the effects of estrogen on cultured hippocampal neurons (Murphy et al., 1998) suggest that estrogen-induced disinhibition is related to subsequent enhancements of excitatory synaptic function, the role of estrogen-induced changes in IPSC kinetics in the downstream effects of estrogen on hippocampal circuitry is not yet known.

References

Alreja M, Wu M, Liu W, Atkins JB, Leranth C, Shanabrough M (2000) Muscarinic tone sustains impulse flow in the septohippocampal GABA but not cholinergic pathway: implications for learning and memory. J Neurosci 20:8103–8110.

Aronica SM, Kraus WL, Katzenellenbogen BS (1994) Estrogen action via the cAMP signaling pathway: stimulation of adenylate cyclase and cAMP-regulated gene transcription. Proc Natl Acad Sci USA 91:8517–8521.

Book AA, Wiley RG, Schweitzer JB (1994) 192 IgG-saporin: I. Specific lethality for cholinergic neurons in the basal forebrain of the rat. J Neuropathol Exp Neurol 53:95–102.

Bradford MM (1976) A rapid and sensitive method for the quantitation of microgram quantities of protein utilizing the principle of protein-dye binding. Anal Biochem 72:248–254.

Brauer K, Seeger G, Hartwig W, Rossner S, Poethke R, Kacza J, Schliebs R, Bruckner, Bigl V (1998) Electron microscopic evidence for a cholinergic innervation of GABAergic parvalbumin-immunoreactive neurons in the rat medial septum. J Neurosci Res 54:248–253.

Buhl EH, Halasy K, Somogyi P (1994) Diverse sources of hippocampal unitary inhibitory postsynaptic potentials and the number of synaptic release sites. Nature 368:823–828.

Daniel JM, Dohanich GP (2001) Acetylcholine mediates the estrogen-induced increase in NMDA receptor binding in CA1 of the hippocampus and the associated improvement in working memory. J Neurosci 21:6949–6956.

DeKosky ST, Scheff SW, Markesbery WR (1985) Laminar organization of cholinergic circuits in human frontal cortex in Alzheimer's disease and aging. Neurology 35:1425–1431.

Freund TF, Antal M (1988) GABA-containing neurons in the septum control inhibitory interneurons in the hippocampus. Nature 336:170–173.

Freund TF, Buzsaki G (1996) Interneurons of the hippocampus. Hippocampus 6:347–470.

Gibbs RB (1996) Fluctuations in relative levels of choline acetyltransferase mRNA in different regions of the rat basal forebrain across the estrous cycle: effects of estrogen and progesterone. J Neurosci 16:1049–1055.

Gibbs RB (1997) Effects of estrogen on basal forebrain cholinergic neurons vary as a function of dose and duration of treatment. Brain Res 757:10–16.

Gibbs RB (2000) Effects of gonadal hormone replacement on measures of basal forebrain cholinergic function. Neuroscience 101:931–938.

Gibbs RB (2002) Basal forebrain cholinergic neurons are necessary for estrogen to enhance acquisition of a delayed matching-to-position T-maze task. Horm Behav 42:245–257.

Gibbs RB, Hashash A, Johnson DA (1997) Effects of estrogen on potassium-stimulated acetylcholine release in the hippocampus and overlying cortex of adult rats. Brain Res 749:143–146.

Hajos N, Papp EC, Acsady L, Levey AI, Freund TF (1998) Distinct interneuron types express m2 muscarinic receptor immunoreactivity on their dendrites or axon terminals in the hippocampus. Neuroscience 82:355–376.

Hart SA, Patton JD, Woolley CS (2001) Quantitative analysis of ERα and GAD colocalization in the hippocampus of the adult female rat. J Comp Neurol 440:144–155.

Hollrigel GS, Soltesz I (1997) Slow kinetics of miniature IPSCs during early postnatal development in granule cells of the dentate gyrus. J Neurosci 17:5119–5128.

Johnson DA, Zambon NJ, Gibbs RB (2002) Selective lesions of cholinergic neurons in the medial septum by 192 IgG-saporin impairs learning in a delayed matching to position T-maze paradigm. Brain Res 943:132–141.

Kunkel DD, Lacaille JC, Schwartzkroin PA (1988) Ultrastructure of stratum lacunosum-moleculare interneurons of the hippocampal CA1 region. Synapse 2:382–394.

Lacaille JC, Schwartzkroin PA (1988) Stratum lacunosum-moleculare interneurons of hippocampal CA1 region. II. Intrasomatic and intradendritic recordings of local circuit synaptic interactions. J Neurosci 8:1411–1424.

Lavoie AM, Tingey JJ. Harrison NL, Pritchett DB, Twyman RE (1997) Activation and deactivation rates of recombinant GABA(A) receptor channels are dependent on alpha-subunit isoform. Biophys J 73:2518–2526.

Luine VN (1985) Estradiol increases choline acetyltranferase activity in specific basal forebrain nuclei and projection areas of female rats. Exp Neurol 89:484–490.

Mermelstein PG, Becker JB, Surmeier DJ (1996) Estradiol reduces calcium currents in rat neostriatal neurons via a membrane receptor. J Neurosci 16:595–604.

Milner TA, McEwen BS, Hayashi S, Li CJ, Reagan LP, Alves SE (2001) Ultrastructural evidence that hippocampal alpha estrogen receptors are located at extranuclear sites. J Comp Neurol 429:355–371.

Morley P, Whitfield JF, Vanderhyden BC, Tsang BK, Schwartz JL (1992) A new, nongenomic estrogen action: the rapid release of intracellular calcium. Endocrinology 131:1305–1312.

Moss RL, Gu Q (1999) Estrogen: mechanisms for a rapid action in CA1 hippocampal neurons. Steroids 64:14–21.

Murphy DD, Cole NB, Greenberger V, Segal M (1998) Estradiol increases dendritic spine density by reducing GABA neurotransmission in hippocampal neurons. J Neurosci 18:2550–2559.

Parducz A, Perez J, Garcia-Segura LM (1993) Estradiol induces plasticity of GABAergic synapses in the hypothalamus. Neuroscience 53:395–401.

Parducz A, Hoyk Z, Kis Z, Garcia-Segura LM (2002) Hormonal enhancement of neuronal firing is linked to structural remodeling of excitatory and inhibitory synapses. Eur J Neurosci 16:665–670.

Paxinos G (1995) The rat nervous system. San Diego: Academic.

Pearce RA (1993) Physiological evidence for two distinct $GABA_A$ responses in rat hippocampus. Neuron 10:189–200.

Rudick CN, Woolley CS (2001) Estrogen regulates functional inhibition of hippocampal CA1 pyramidal cells in the adult female rat. J Neurosci 21:6532–6543.

Rudick CN, Woolley CS (2003) Selective estrogen receptor modulators regulate phasic activation of hippocampal CA1 pyramidal cells by estrogen. Endocrinology 144:179–187.

Sandstrom NJ, Williams CL (2001) Memory retention is modulated by acute estradiol and progesterone replacement. Behav Neurosci 115:384–393.

Shughrue PJ, Scrimo PJ, Merchenthaler I (2000) Estrogen binding and estrogen receptor characterization (ERalpha and ERbeta) in the cholinergic neurons of the rat basal forebrain. Neuroscience 96:41–49.

Smith SS, Gong QH, Hsu FC, Markowitz RS, ffrench-Mullen MH, Li X (1998) $GABA_A$ receptor α4 subunit suppression prevents withdrawal properties of an endogenous steroid. Nature 392:926–930.

Thompson SM, Gahwiler BH (1992) Effects of the GABA uptake inhibitor tiagabine on inhibitory synaptic potentials in rat hippocampal slice cultures. J Neurophysiol 67:1698–1701.

Watters JJ, Dorsa DM (1998) Transcriptional effects of estrogen neuronal neurotensin gene expression involve cAMP/protein kinase A-dependent signaling mechanisms. J Neurosci 18:6672–6680.

Woolley CS, McEwen BS (1992) Estradiol mediates fluctuation in hippocampal synapse density during the estrous cycle in the adult rat. J Neurosci 12:2549–2554.